SUPPLEMENTAL

Quantifying the spatiotemporal variability in zooplankton dynamics in the Gulf of Mexico using a physical-biogeochemical model

S1 Biogeochemical model forcing, initial, and open boundary conditions

Surface downward shortwave radiation fields provided by the National Centers for Environmental Prediction (NCEP) were used to estimate light limitation of phytoplankton in NEMURO-GoM. Specifically, Climate Forecast System Reanalysis (CFSR) hourly shortwave radiation fields were daily averaged and used to force the model from 1993 to 2010. CFSv2 fields were also daily averaged and used for the remaining two years of the simulation. Before use in the model both CFSR (~38km resolution) and CFSv2 (~34.5 km resolution) products were linearly interpolated to the NEMURO-GoM grid (~20 km) and subsequently scaled by a factor of 0.43 (default NEMURO parameter) to estimate photosynthetic active radiation (PAR) which is used directly in the SP and LP light limitation term to estimate phytoplankton growth rates.

In total, the online H-GoM simulation that provided flow fields for NEMURO-GoM incorporated 37 independent rivers with climatological monthly averaged discharge. These same river locations and discharges were used along with nutrient measurements to prescribe riverine nutrient input in the offline NEMURO-GoM. Due to a lack of water quality data the same nutrient time series derived for the Mississippi River was prescribed for all rivers. Nutrient input associated with Mississippi river discharged into the GoM was approximated using data from United States Geological Survey (USGS) real-time streamflow and water quality analysis at station 07374000 (Baton Rouge, LA). Climatological daily averaged nitrate concentrations were derived from USGS samples collected from 2011 to 2017. The daily climatology was then use cyclically in NEMURO-GoM for all 20 years of the simulation. Silica river input was approximated using a constant Si:N ratio of 2.0. We found that adding additional sources of nitrogen equivalent to 10% of the USGS daily nitrate concentration for the remaining four nutrient pools (i.e. NH, DON, PON, and OP) had no appreciable impact on the model.

Initial and open boundary conditions for all eleven NEMURO state variables were derived from an idealized one-dimensional model version of NEMURO-GoM (see **S3** for more details on the one-dimensional model). An annual averaged profile for all state variables was determined from the one-dimensional model and prescribed throughout the domain which served as an initial condition. The same profile was applied at the boundaries. The open boundary condition in NEMURO-GoM was held constant for all 20-years. This is likely a reasonable assumption given the lack of seasonality south of the domain. Additionally, there is minimal impact of the western and northern boundary on the GoM. Prior to integrating NEMURO-GoM from 1993-2012 the model was spun up for a total of four years with daily flow fields from 1993. The spun up state variable fields were subsequently used as the new initial condition for the full 20-year NEMURO-GoM simulation. Model output south of 21°N and west of the Mexico coastline as well as east of 81°W was considered a boundary buffer zone and excluded from model-data comparisons.

S2 NEMURO modifications

To increase realism of NEMURO's application to the GoM we implemented a total of five formulation changes to the original NEMURO code. We justify the changes in detail in the manuscript (see section 2.1.2) but for reference we briefly state them again here. The most substantial change was our choice to remove LZ grazing on SP. This modification was motivated by the significant taxonomic differences that are found between mesozooplankton communities and their prey in the GoM and the North Pacific. Next, we chose to implement linear mortality on all biological state variables with the exception of PZ. This was done because predation is already explicitly modeled on all biological state variables apart from PZ. We also implemented a more widely adopted ammonium inhibition term (with monotonic behavior) and light limitation functional form (with an explicit photoinhibition parameter). Lastly, we added a variable C:Chl model based on Li et al. (2010). We chose to implement this model to account for changes in phytoplankton cellular C:Chl as a response to varying nutrient and light conditions, and because it was developed specifically for use in NEMURO.

The Li et al. (2010) model was originally parameterized based on field data from the California Current (CC). For application to the GoM we increased phytoplankton C:Chl by decreasing the

maximum Chl:C parameter values by 50%. Our motivation behind this modification was associated with the significant oceanographic differences that exist between the GoM and CC. The CC is a region characterized by strong upwelling where near surface nutrient concentrations are significantly higher than typically found in the GoM, particularly in offshore regions. Concurrently, light levels are lower in the CC due to both higher phytoplankton biomass and decreased sunlight at higher latitudes. Such conditions can support phytoplankton communities with C:Chl ratios that are much lower than one would expect to find in the tropical highly oligotrophic GoM. During the NEMURO-GoM integration we found that the original Li et al. (2010) model estimated C:Chl ratios in the oligotrophic region of ~35 and ~20 on average for SP and LP, respectively. After our modification C:Chl ratios in NEMURO-GoM were on average ~70 for SP and ~40 for LP which more closely compares with values of ~80 in recent samples collected during May 2017/2018 oligotrophic GoM cruises. The variable Chl:C model, ammonium inhibition term, and light formulation change are considered "default" NEMURO herein. Through the tuning process we evaluated the impact of the two additional changes (i.e. removal of SP to LZ grazing pathway and linear mortality).

S3 NEMURO parameter tuning

In this section the motivation and progression of tuning NEMRURO for its application to the GoM is outlined. We considered five main ecosystem benchmarks during the tuning process: surface Chl, depth averaged mesozooplankton biomass, DCM depth, DCM magnitude, and LP relative abundance (i.e. LP/(SP+LP)). Surface Chl and mesozooplankton biomass were chosen as benchmarks to evaluate model skill in estimating the distribution of plankton biomass. DCM depth and magnitude were chosen to provide a baseline to evaluate the vertical structure of the simulated ecosystem. Finally, LP relative abundance was chosen as a benchmark to evaluate the realism of simulated phytoplankton communities under different nutrient conditions (e.g. shelf vs oligotrophic). A full summary of parameter changes and their resulting impacts in the one-dimensional model can be found in **Table S1.** All parameter values used in the present study can be found in **Table S2**. Given the computational demands of running the three-dimensional model our initial parameter tuning was carried out in the idealized one-dimensional model version of NEMURO-GoM. A description of the one-dimensional model is presented below.

The one-dimensional model was designed and written in Matlab. The model closely mimics NEMURO-GoM and has the same 29 z-levels. The one-dimensional model can be downloaded from GitHub at https://github.com/. To generate initial condition profiles for the one-dimensional model we utilized nitrate and silicate data collected in the oligotrophic GoM and provided from World Ocean Atlas. All other state variables were set to a constant value of 0.01 mmol N m^{-3}. The one-dimensional model was run for two years and forced with daily photosynthetically active radiation (PAR) and temperature profiles derived from the same fields prescribed during the NEMURO-GoM integration. Daily PAR and temperature profiles were calculated from a spatial average over a 2° x 2° sample box located in the oligotrophic GoM with an origin at 24° N, 91° W. To simulate the vertical motion (w-velocity + vertical diffusivity) in the one-dimensional model a constant vertical diffusivity was implemented. We found that a vertical diffusivity of $1.75x10^{-4}$ m^2 s^{-1} produced a similar average nitracline between the one-dimensional and the three-dimensional model. Ecosystem responses to parameter changes for shelf conditions were explored by holding surface nitrate and silicate values constant to mimic riverine input. We found that ecosystem responses due to parameter modifications in the one-dimensional model were closely mirrored in the three-dimensional model which enabled efficient parameter tuning.

Table S1: The impact of key ecosystem characteristics during the parameter tuning process is displayed below. Results are from an idealized one-dimensional version of NEMURO-GoM. Ecosystem benchmarks include surface Chl (mg Chl m^{-3}), 200m depth averaged mesozooplankton biomass. (MZB, mmol N m^{-3}), DCM depth (m), DCM magnitude (m), and LP dominance (%).

Parameter Modification	**Surface Chl**	**MZB**	**DCM**	**DCM Magnitude**	**LP Abundance**
Target	0.12	0.045	80	0.6	<40% / >60%
NEMURO (Kishi et al., 2007)	0.29	0.091	25	0.6	23% / 18%
Default NEMURO	0.42	0.082	25	0.6	17% / 19%
Decrease implicit bacterial rates	0.24	0.067	35	0.4	23% / 20%
SP & LP A = 0.1	0.07	0.091	75	0.5	41% / 21%
Attenuation = 0.03	0.04	0.098	105	0.6	24% / 21%
Implemented linear mortality	0.01	0.061	105	0.7	13% / 8%
Decrease phytoplankton mortality	0.05	0.081	105	0.7	12% / 3%
Increase zooplankton mortality	0.06	0.036	105	0.7	6% / 0.5%
Sinking = 15	0.12	0.060	95	1.0	18% / 0.3%
Removal of SP2LZ	0.12	0.053	95	1.0	21% / 4%
SP2SZ = 0.5	0.12	0.054	95	0.7	27% / 14%
LP & SZ2LZ = 0.3	0.12	0.055	95	0.8	29% / 28%
LP & SZ2PZ = 0.1; LZ2PZ = 0.3	0.14	0.041	95	0.8	37% / 52%

SP2SZ = 0.6	0.13	0.041	85	0.5	41% / 77%
SP NO_3 Half Situation = 0.5	0.13	0.041	85	0.7	39% / 61%
Si/N = 1.0	0.14	0.049	85	0.6	42% / 77%
20 Year Average (3D Model)	0.12	0.043	85	0.6	32% / 93%

When implementing default NEMURO parameter values in the one-dimensional model and in the three-dimensional model we quickly found that nutrient cycling occurred too rapidly in the surface ocean. To achieve realistic surface Chl fields C:Chl ratios needed to be greater than 200 indicating that the default NEMURO parameter set produced unrealistically high phytoplankton biomass. Our initial suspicions of high nutrient cycling became apparent when looking at daily bacterial rates estimated by the one-dimensional model. Using the default NEMURO parameter value for the remineralization of DON to NH_4 resulted in 100% d^{-1} of the DON pool being remineralized (at 25°C – an average GoM SST) over the course of a single day ($DON2NH_4$= exp(0.0693*25)*0.2 = 1.13). Hence, we modified the five temperature dependent parameters responsible for implicit bacterial remineralization and nitrification.

In reducing these bacterial parameters values by an order of magnitude the one-dimensional model estimated average concentrations of surface nitrate (<0.1 mmol N^{-3}) and Chl (0.24 mg Chl m^{-3}), while still high, fell within the range of realistic values found in the oligotrophic GoM (surface Chl during winter is typically 0.2 – 0.25 mg Chl m^{-3}). The reduced implicit bacterial rates used here are comparable to values used in previous GoM studies (Damien et al., 2018; Fennel et al., 2006; Gomez et al., 2018). After lowering the implicit bacterial rates by an order of magnitude the remineralization of DON to NH_4 becomes 0.02 (11% d^{-1} at 25°C) which is similar to Gomez et al. (2018) parameter value of 0.0071 (4% d^{-1} at 25°C). The decomposition of opal to SiO^{4-} by default is set to 0.1 which resulted in an unrealistically high remineralization rate (56% d^{-1} at 25°C). Here we use a value of 0.01 (5.6% d^{-1} at 25°C) which is also comparable to that of Gomez et al. (2018) who implemented a parameter value of 0.0035 (2% d^{-1} at 25°C). Other bacterial rates such as nitrification are similarly parameterized with values of 1-5% d^{-1} (Fennel et al., 2011). Here nitrification is set to 0.003 (2% d^{-1} at 25°C) and the remineralization of PON to NH_4 is set to 0.01 (5.6% d^{-1} at 25°C).

One exception to our modification of the implicit bacterial rates is the decomposition of PON to DON. When implementing the parameter changes in the three-dimensional model we found that decreasing the decomposition of PON by a full order of magnitude led to excessive PON retention on the shelf. This resulted in model estimates of phytoplankton and zooplankton biomass that were substantially higher than observed values in the shelf region as well as biomass estimates that were substantially lower than observed values in the oligotrophic region. We also noticed that the offshore to onshore gradient in simulated surface Chl was much sharper than found in seaWIFS fields. We achieved more realistic surface Chl fields by only reducing PON decomposition by 50%.

While changes to the implicit bacterial rates enabled the one-dimensional model to estimate reasonable surface concentrations, the model still produced nitracline and DCM depths that were unrealistically shallow. Based on 36 nitrate profiles measured in the oligotrophic GoM during May 2017 and 2018 cruise we found that nitrate was typically undetectable above 100 m. We also found associated DCM depths of 80-140 m. Similarly, DCM depths were on average 80 $\pm$ 25 m in 1402 fluorescence profiles taken in the oligotrophic region during the SEAMAP surveys. By stark contrast, we found that simulated nitracline depths were on average ~10 m with a DCM at ~25 m in the one-dimensional model. We also found this was true in the three-dimensional model which resulted in an over estimation of surface nutrient concentrations and Chl within strong divergent flows, particularly north of the Yucatan peninsula. Increasing the parameter α (i.e. slope of the photosynthesis-irradiance curve) by an order of magnitude allowed phytoplankton to grow more effectively at depth and subsequently draw down nutrient concentrations in the mixed layer. This resulted in a more realistic simulated nitracline (~50 m) and DCM depth (~70 m). The value of 0.1 used here for α is similar to 0.125 implemented by (Fennel et al., 2006, 2011). Values of α as high as 0.5 have been used in the GoM by Damien et al. (2018). In an effort to deepen the DCM further we reduced the attenuation coefficient due to water and phytoplankton from 0.04 to 0.03. With this change the one-dimensional model estimated average nitracline and DCM depths of ~90 and ~100 m respectively. Attenuation coefficients below 0.04 were similarly used by Gomez et al. (2018). Reducing the attention coefficients also provided more realistic euphotic zone depths (i.e. 1% surface irradiance) in the model. Euphotic zone depth increased from 85 m to 115 m which

more closely agreed with CTD casts conducted during a 2017 and 2018 cruise where we observed euphotic zone depths greater than 100 m.

With modifications to implicit bacterial rates, light parameter α, and the attenuation coefficients, the one-dimensional model produced reasonable estimates of plankton biomass at depth. However, simulated surface Chl was now lower than observed by a factor of approximately 3.0 which was due in part to high zooplankton biomass and hence strong grazing pressure. Up to this point in the tuning process the one-dimensional model overestimated mesozooplankton biomass (i.e. LZ+PZ) relative to SEAMAP samples in the oligotrophic GoM by a factor of 2.0 – 3.0 even with substantially lower than observed surface Chl. Model estimates for mesozooplankton biomass were on average ~8 mg C m^{-3} compared to average SEAMAP measurements of ~3.5 mg C m^{-3} in the oligotrophic GoM. After closer inspection we found that high mesozooplankton biomass could be attributed to the default NEMURO quadratic mortality term which effectively increases biomass lower limits by reducing mortality rates at low biomass. We found mortality parameter values for LZ and PZ had to be increased by an order of magnitude to simulate mesozooplankton biomass low enough to compare well with SEAMAP observations in the oligotrophic region. Instead, we chose to implement a linear mortality formulation on all biological state variables with the exception of PZ to achieve lower limits of mesozooplankton biomass. Quadratic mortality was retained for PZ to simulate the implicit predation of un-modeled higher trophic levels.

A linear mortality parameter value of 0.0109 d^{-1} was used as an equivalent to the default quadratic mortality parameter (i.e. 0.0585 d^{-1}) and served as a baseline for model tuning. The value results in the same mortality rate as the quadratic term (at 25°C with an average plankton biomass). A similar value was used in Gomez et al. (2018) where a value of 0.016 d^{-1} was implemented for both SP and LP mortality. However, we found that a mortality value of 0.0109 d^{-1} was too high for phytoplankton in the one-dimensional simulations and accounted for up to 40% of the gross primary production (GPP). By lowering the mortality value by a factor of 5.0 the model estimated more realistic surface phytoplankton biomass and mortality losses (<10% GPP). We note that our phytoplankton mortality parameter value needed to be substantially lower relative to previous studies because NEMURO explicitly includes mortality, respiration, and extracellular excretion as

separate terms which in previous models are often assumed to be combined into a single loss term (e.g. respiration and mortality are combined in Gomez et al. (2018)).

Although we found that mesozooplankton biomas lowered by 20% with the implementation of linear mortality (~6.4 mg C m^{-3}) the one-dimensional model still overestimated mesozooplankton biomass in the oligotrophic GoM by about a factor of 2.0. Hence, we decided to double all zooplankton mortality parameter values (SZ, LZ = 0.022 d^{-1}; PZ = 0.12 d^{-1}). Similar values were implemented in Gomez et al. (2018) where SZ and LZ was set to 0.023 d^{-1} and 0.030 d^{-1} respectively. After increasing the zooplankton mortality values the one-dimensional model now estimate more realistic mesozooplankton biomass but predicted low surface Chl (Model: 0.065 mg Chl m^{-3} vs. seaWIFS: 0.12 mg Chl m^{-3}).

To increase simulated phytoplankton biomass we lowered the sinking rate of PON and OP from 40 m d^{-1} to 15 m d^{-1}. This value is more comparable to previous GoM studies (Gomez et al., 2018) where values as low as 1 m/d have been used (Fennel et al., 2006). Given the smaller size of phytoplankton and zooplankton typically found in lower latitude regional oceans like the GoM it is likely that sinking rates of dead cells (which is one source of PON and OP in our model) would be relatively lower on average compared to sinking rates of dead phytoplankton in the North Pacific where cells are generally larger. Furthermore, we note that since NEMURO has only one detrital pool, this sinking rate must represents a bulk settling velocity for a heterogeneous class of non-living particles and aggregates that in reality range in sinking speeds from negligible to >100 m d^{-1} (Stukel et al., 2014). Lowering sinking rates also allowed more cross shelf transport of nutrients. This was similar to the effect of modifying the PON to DON bacterial decomposition rate. Decreasing sinking rates effectively increased biomass in the oligotrophic GoM and decreased biomass on the shelf. When sinking rates were high in the model, PON quickly reached the bottom over the shelf where currents are typically slower relative to the surface leading to excessive PON retention which lead to high ammonium concentrations. This change was important for places like the Campeche Bank where we found it difficult to lower phytoplankton biomass in NEMURO-GoM.

At this point in the model tuning process the one-dimensional model estimated reasonable ranges of total phytoplankton and zooplankton biomass. This was also true when the parameter changes outlined thus far were implemented into the three-dimensional model. However, we noticed in both the one-dimensional model (when surface nitrate/silicate were held constant) and in three-dimensional model (in the shelf region) the simulated phytoplankton community was noticeably unrealistic. In the ocean, LP are known to generally dominate eutrophic shelf waters as a result of higher maximum growth rates and the ability to escape protistan grazing pressure while SP outcompete LP in oligotrophic waters as a result of their lower surface area to volume ratios and commensurate competitive advantages when nutrients are severely limiting. One would expect to see some dominance in the model of LP on the GoM shelf especially near the Mississippi River mouth. Yet, in both the default NEMURO parameter set and the parameter modifications presented thus far both the one-dimensional and three-dimensional model produced a phytoplankton community with strong SP dominance making up more than 80% of total phytoplankton biomass throughout the domain and during all four seasons. We found that adjusting nutrient half saturation constants within reasonable values for both coastal and offshore phytoplankton communities was not enough to produce a realistic phytoplankton community. We also tried increasing LP maximum growth rate and decreasing SP maximum growth rate. Even with the same half saturation constants and no silica limitation these parameter changes did not substantially change LP relative abundance (<10% on the shelf) suggesting that grazing pressure was too high on LP. Therefore, next we modified the default maximum zooplankton grazing rates. In future studies it would be useful to include two SP and two LP functional types to better parameterize shelf and oligotrophic phytoplankton communities.

In an effort to lower the grazing pressure on LP and to make them more competitive throughout the model we collectively modified all maximum zooplankton grazing rates by a constant value of ± 0.1 d^{-1}. First, we increased SZ grazing on SP which effectively decreased SP abundance everywhere in the model. We then decreased LZ and PZ grazing on SZ to further increase grazing pressure on SP. By contrast, we lowered grazing pressure on LP by reducing LZ and PZ maximum grazing rates on LP. Lastly, we increased PZ "grazing" pressure on LZ which subsequently reduced grazing pressure on SZ and LP, thus allowing for decreases in SP and increases in LP biomass. We note that changes to SZ, LZ, and PZ grazing rates in isolation were inadequate to

allow for LP dominance on the shelf. We also note that the removal of LZ grazing on SP aided the model in allowing greater LP dominance. Despite intuition, we found that LZ grazing on SP sustained LZ to an extent where they could effectively graze down LP.

These grazing rate modifications resulted in LP weakly dominating (~50-60% of the total phytoplankton community) on the shelf. We found that an additional 0.1 increase in SZ grazing rate resulted in higher LP relative abundance (~70-80%). Increasing SZ grazing to 0.6 also helped the model to simulate lower, more realistic, chlorophyll concentrations at the DCM. However, changes in grazing rates had the undesired effect of substantially decreasing SP dominance to around 50-60% in the oligotrophic GoM. We decided to compensate this by decreasing the nitrate half saturation constant of SP by a factor of 2.0. The same half saturation value for nitrate was used by Fennel et al. (2011).

Finally, the last parameter modification was made to the Si:N ratio. Here we use a value of 1.0, which more accurately reflects typical diatom Si:N ratio (Brzezinski, 1985). We found that this modification allowed LP to outcompete SP at depth in the oligotrophic GoM. For similar reasons to the existence of LP dominance on the shelf, one would expect to find smaller cells near the surface and at least a higher proportion of large cells near the DCM. However, with the default Si:N ratio we noticed that SP always outcompeted LP at depth and the proportion of LP did not significantly increase with depth. After implementing the parameter modifications detailed above the one-dimensional model and NEMURO-GoM estimated realistic (1) surface Chl, (2) DCM depth, (3) DCM magnitude, (4) mesozooplankton biomass, and (5) LP relative abundance.

S4 Biogeochemical model parameter values

Table S2: Values and description for all model parameters.

Parameter		Units	Default	PBM
Small Phytoplankton				
V_{SP}	Maximum growth rate at 0 °C	d^{-1}	0.4	0.4
K_{NO2SP}	Nitrate half saturation constant	mmol N m^{-3}	1.0	0.5
K_{NH2SP}	Ammonium half saturation constant	mmol N m^{-3}	0.1	0.1
α_{SP}	Initial slope of the P-I curve	m^2 W^{-1} d^{-1}	0.01	0.1
β_{SP}	Photo inhibition	m^2 W^{-1} d^{-1}	$4.5e^{-4}$	$4.5e^{-4}$
R_{SP}	Respiration at 0 °C	d^{-1}	0.03	0.03

M_{SP}	Mortality at 0 °C	d^{-1}	0.0585	0.002
E_{SP}	Extracellular excretion	Non-Dim.	0.135	0.135
Q_{VSP}	Growth temperature dependence	$°C^{-1}$	0.0693	0.0693
Q_{RSP}	Respiration temperature dependence	$°C^{-1}$	0.0693	0.0693
Q_{MSP}	Mortality temperature dependence	$°C^{-1}$	0.0693	0.0693
Large Phytoplankton				
V_{LP}	Maximum growth rate at 0 °C	d^{-1}	0.8	0.8
K_{NO2LP}	Nitrate half saturation constant	mmol N m^{-3}	3.0	3.0
K_{NH2LP}	Ammonium half saturation constant	mmol N m^{-3}	0.3	0.3
K_{SI}	Ammonium half saturation constant	mmol N m^{-3}	6.0	6.0
α_{LP}	Initial slope of the P-I curve	m^2 W^{-1} d^{-1}	0.01	0.1
β_{LP}	Photo inhibition	m^2 W^{-1} d^{-1}	$4.5e^{-4}$	$4.5e^{-4}$
R_{LP}	Respiration at 0 °C	d^{-1}	0.3	0.03
M_{LP}	Mortality at 0 °C	d^{-1}	0.029	0.001
E_{LP}	Extracellular excretion	Non-Dim.	0.135	0.135
Q_{VLP}	Growth temperature dependence	$°C^{-1}$	0.0693	0.0693
Q_{RLP}	Mortality temperature dependence	$°C^{-1}$	0.0693	0.0693
Q_{MLP}	Respiration temperature dependence	$°C^{-1}$	0.0693	0.0693
Small Zooplankton				
G_{SP2SZ}	Maximum grazing rate on SP at 0 °C	d^{-1}	0.4	0.6
φ_{SP2SZ}	Ivlev grazing constant	m^3 mmol N^{-1}	1.4	1.4
τ_{SP2SZ}	Grazing threshold for feeding on SP	mmol N m^{-3}	0.043	0.04
AE_{SZ}	Assimilation efficiency	Non-Dim.	0.7	0.7
GGE_{SZ}	Gross growth efficiency	Non-Dim.	0.3	0.3
M_{SZ}	Mortality at 0 °C	d^{-1}	0.0585	0.022
Q_{GSZ}	SZ grazing temperature dependence	$°C^{-1}$	0.0693	0.0693
Q_{MSZ}	Mortality temperature dependence	$°C^{-1}$	0.0693	0.0693
Large Zooplankton				
G_{SP2LZ}	Maximum grazing rate on SP at 0 °C	d^{-1}	0.1	0.0
G_{SP2LZ}	Maximum grazing rate on LP at 0 °C	d^{-1}	0.4	0.3
G_{SP2LZ}	Maximum grazing rate on SZ at 0 °C	d^{-1}	0.4	0.3
φ_{LP2LZ}	Ivlev grazing constant	m^3 mmol N^{-1}	1.4	1.4
φ_{SZ2LZ}	Ivlev grazing constant	m^3 mmol N^{-1}	1.4	1.4
τ_{LP2LZ}	Grazing threshold for feeding on LP	mmol N m^{-3}	0.04	0.04
τ_{SZ2LZ}	Grazing threshold for feeding on SZ	mmol N m^{-3}	0.04	0.04
AE_{LZ}	Assimilation efficiency	Non-Dim.	0.7	0.7
GGE_{LZ}	Gross growth efficiency	Non-Dim.	0.3	0.3
M_{LZ}	Mortality at 0 °C	d^{-1}	0.0585	0.022
Q_{GLZ}	LZ grazing temperature dependence	$°C^{-1}$	0.0693	0.0693
Q_{MLZ}	Mortality temperature dependence	$°C^{-1}$	0.0693	0.0693
Predatory Zooplankton				
G_{SP2LZ}	Maximum grazing rate on LP at 0 °C	d^{-1}	0.2	0.1
G_{SP2LZ}	Maximum grazing rate on SZ at 0 °C	d^{-1}	0.2	0.1
G_{SP2LZ}	Maximum grazing rate on LZat 0 °C	d^{-1}	0.2	0.3
φ_{LP2LZ}	Ivlev grazing constant	m^3 mmol N^{-1}	1.4	1.4
φ_{SZ2LZ}	Ivlev grazing constant	m^3 mmol N^{-1}	1.4	1.4
φ_{SZ2LZ}	Ivlev grazing constant	m^3 mmol N^{-1}	1.4	1.4
τ_{LP2LZ}	Grazing threshold for feeding on LP	mmol N m^{-3}	0.04	0.04
τ_{SZ2LZ}	Grazing threshold for feeding on SZ	mmol N m^{-3}	0.04	0.04

τ_{SZ2LZ}	Grazing threshold for feeding on LZ	mmol N m^{-3}	0.04	0.04
AE_{LZ}	Assimilation efficiency	Non-Dim.	0.7	0.7
GGE_{LZ}	Gross growth efficiency	Non-Dim.	0.3	0.3
M_{LZ}	Mortality at 0 °C	d^{-1}	0.0585	0.12
Q_{GLZ}	PZ grazing temperature dependence	$°C^{-1}$	0.0693	0.0693
Q_{MLZ}	Mortality temperature dependence	$°C^{-1}$	0.0693	0.0693
λ_{SZLZ}	SZ and LZ inhibition on LP	m^3 mmol N^{-1}	4.605	4.605
λ_{LZ}	LZ inhibition on SZ	m^3 mmol N^{-1}	3.01	3.01
Implicit Bacterial Rates				
B_{NIT}	Nitrification at 0 °C	d^{-1}	0.03	0.003
B_{PON2NH}	PON decomposition to NH_4 at 0 °C	d^{-1}	0.1	0.01
$B_{PON2DON}$	PON decomposition to DON at 0 °C	d^{-1}	0.1	0.05
B_{DON2NH}	DON decomposition to NH_4 at 0 °C	d^{-1}	0.2	0.02
B_{OP2SI}	Opal decomposition to Silica at 0 °C	d^{-1}	0.1	0.01
Q_{NIT}	Nitrification	$°C^{-1}$	0.0693	0.0693
Q_{PON2NH}	PON2NH temperature dependence	$°C^{-1}$	0.0693	0.0693
$Q_{PON2DON}$	PON2DON temperature dependence	$°C^{-1}$	0.0693	0.0693
Q_{NIT}	DON2NH temperature dependence	$°C^{-1}$	0.0693	0.0693
Q_{NIT}	OP2SI temperature dependence	$°C^{-1}$	0.0693	0.0693
Other NEMURO Parameters				
ε_W	Attenuation of light due to water	m^{-1}	0.04	0.03
ε_{SP}	Attenuation of light due to SP	m^2 mmol N^{-1}	0.04	0.03
ε_{LP}	Attenuation of light due to LP	m^2 mmol N^{-1}	0.04	0.03
PAR	Photosynthetically active radiation	Non-Dim.	0.43	0.43
$Si:N$	Ratio of Silica to Nitrogen	mmol Si mmol N^{-1}	2.0	1.0
Ω	Sinking speed of PON and OP	m d^{-1}	40	15
$Si:N_{riv}$	Ratio of Silica to Nitrogen in river water	mmol Si mmol N^{-1}	N/A	2.0
Variable Chl:C Sub-Model				
$Chl2C_{SPmin}$	Minimum SP Chl:C ratio	mg Chl mg C^{-1}	0.000	0.0000
$Chl2C_{LPmin}$	Minimum LP Chl:C ratio	mg Chl mg C^{-1}	0.005	0.005
$Chl2C_{SPmax}$	Maximum SP Chl:C ratio	mg Chl mg C^{-1}	0.030	0.015
$Chl2C_{LPmax}$	Maximum LP Chl:C ratio	mg Chl mg C^{-1}	0.061	0.03
α_{chl}	Chl specific initial slope of P-I curve	mg C mg Chl^{-1}	0.28	0.28

S5 Parameter Sensitivity Experiments

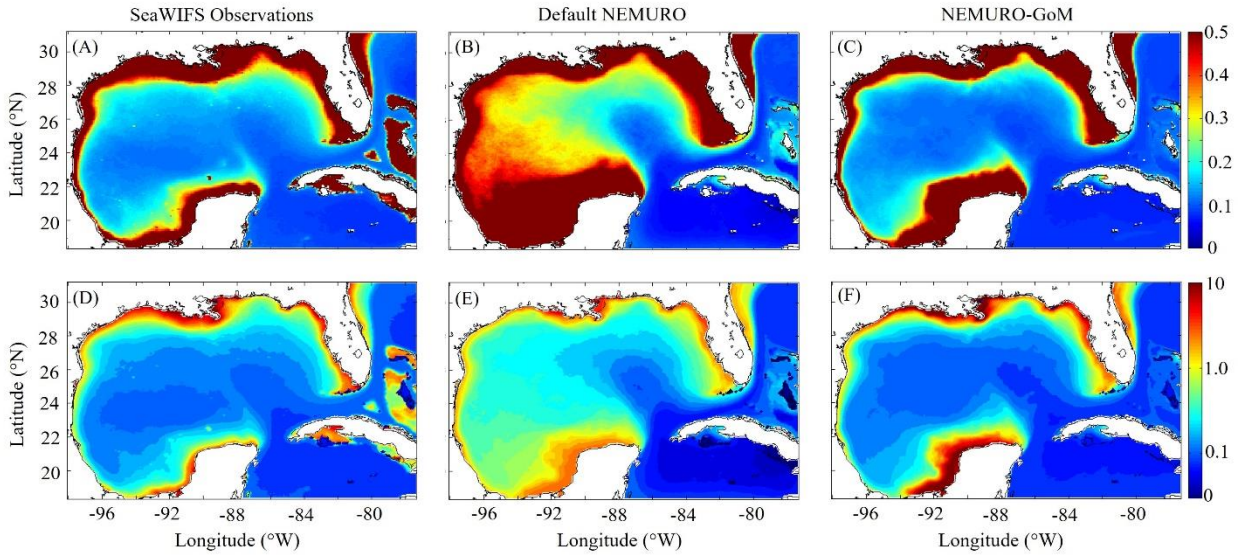

Figure S1: Climatological surface chlorophyll (mg Chl m^{-3}) based on SeaWIFS (A), default NEMURO (B), the tunned NEMURO-GoM (C) with their respective $\log_{10}$ field (D-F) below.

Table S3: Configuration of parameter sensitivity experiments and the average values for surface Chl (mg Chl m^{-3}), depth averaged mesozooplankton biomass (MZB, mmol N m^{-3}), and deep chlorophyll maximum depth (DCM, m) for the oligotrophic region (bathymetry ≥1000 m).

Expt #	Configuration	Surface Chl	MZB	DCM Depth
	Observations (1993-2012)	0.129	0.044	81
	Default NEMURO	0.225	0.057	40
	NEMURO-GoM	0.117	0.049	96
	Observations (2002-2005)	0.126	0.049	62
1	Default NEMURO	0.213	0.053	40
2	NEMURO-GoM (NG)	0.120	0.053	82
3	NG + Default SP2LZ	0.117	0.059	81
4	NG + Default quadratic mortality	0.086	0.101	83
5	NG + Default phytoplankton alpha	0.224	0.022	52
6	NG + Default attenuation coefficients	0.147	0.035	68
7	NG + Default sinking	0.089	0.048	84
8	NG + Default SP NO_3 K_s	0.123	0.053	81
9	NG + Default SP2SZ	0.135	0.049	82
10	NG + Default LP2LZ & SZ2LZ	0.117	0.054	81
11	NG + Default LP2PZ & SZ2PZ	0.117	0.059	82
12	NG + Default LZ2PZ	0.121	0.055	81
13	NG + Default nitrification	0.117	0.053	81
14	NG + Default PON2NH	0.152	0.061	79

15	NG + Default DON2NH	0.099	0.055	82
16	NG + Default PON2DON	0.144	0.057	80
17	NG + Default OP2SI	0.141	0.060	80
18	NG + Default Si/N	0.105	0.048	85

S6 NEMURO biogeochemical model equations

Model state variables:

SP	Small phytoplankton (picoplankton)
LP	Large phytoplankton (nanoplankton)
SZ	Small zooplankton (heterotrophic protistian zooplankton)
LZ	Large zooplankton (suspension feeding mesozooplankton)
PZ	Predatory zooplankton (predatory mesozooplankton)
NO	Nitrate (NO_3)
NH	Ammonium (NH_4)
SI	Silicate (SiO^{4-})
DON	Dissolved organic nutrients
PON	Particulate organic nutrients
OP	Opal

Simulated ecosystem processes:

GPP_{NO2SP}	Small phytoplankton gross primary production supported by NO_3
GPP_{NH2SP}	Small phytoplankton gross primary production supported by NH_4
GPP_{NO2LP}	Large phytoplankton gross primary production supported by NO_3
GPP_{NH2LP}	Large phytoplankton gross primary production supported by NH_4
RES_{SP}	Small phytoplankton respiration
RES_{LP}	Large phytoplankton respiration
MOR_{SP}	Small phytoplankton linear mortality
MOR_{LP}	Large phytoplankton linear mortality
EXC_{SP}	Small phytoplankton extracellular excretion
EXC_{LP}	Large phytoplankton extracellular excretion
GRA_{SP2SZ}	Small phytoplankton loss due to small zooplankton grazing

GRA_{LP2LZ}	Large phytoplankton loss due to large zooplankton grazing
GRA_{LP2PZ}	Large phytoplankton loss due to predatory zooplankton grazing
GRA_{SZ2LZ}	Small zooplankton loss due to large zooplankton predation
GRA_{SZ2PZ}	Small zooplankton loss due to predatory zooplankton predation
GRA_{LZ2PZ}	Large zooplankton loss due to predatory zooplankton predation
MOR_{SZ}	Small zooplankton linear mortality
MOR_{LZ}	Large zooplankton linear mortality
MOR_{PZ}	Predatory zooplankton quadratic mortality
EXR_{SZ}	Total small zooplankton excretion
EXR_{LZ}	Total large zooplankton excretion
EXR_{PZ}	Total predatory zooplankton excretion
EGE_{SZ}	Total small zooplankton egestion
EGE_{LZ}	Total large zooplankton egestion
EGE_{PZ}	Total predatory zooplankton egestion
NIT	Implicit bacterial nitrification
PON2NH	Implicit bacterial remineralization of PON to NH_4
PON2DON	Implicit bacterial decomposition of PON to DON
DON2NH	Implicit bacterial remineralization of DON to NH_4
OP2SI	Implicit bacterial remineralization of OP to SiO^{4-}

State variable differential equations:

$$\frac{d(SP)}{dt} = GPP_{NO2SP} + GPP_{NH2SP} - RES_{SP} - EXC_{SP} - MOR_{SP} - GRA_{SP2SZ}$$

$$\frac{d(LP)}{dt} = GPP_{NO2LP} + GPP_{NH2LP} - RES_{LP} - EXC_{LP} - MOR_{LP} - GRA_{LP2LZ} - GRA_{LP2PZ}$$

$$\frac{d(SZ)}{dt} = GRA_{SP2SZ} \times GGE_{SZ} - MOR_{SZ} - EXR_{SZ} - EGE_{SZ} - GRA_{SZ2LZ} - GRZ_{SZ2PZ}$$

$$\frac{d(LZ)}{dt} = (GRA_{LP2LZ} + GRA_{SZ2LZ}) \times GGE_{LZ} - MOR_{LZ} - EXR_{LZ} - EGE_{LZ} - GRA_{LZ2LPZ}$$

$$\frac{d(PZ)}{dt} = (GRA_{LP2PZ} + GRA_{SZ2PZ} + GRA_{LZ2PZ}) \times GGE_{PZ} - MOR_{PZ} - EXR_{PZ} - EGE_{PZ}$$

$$\frac{d(NO)}{dt} = NIT + RES_{SP} \times \left(\frac{GPP_{NO2SP}}{GPP_{SP}}\right) + RES_{SP} \times \left(\frac{GPP_{NO2LP}}{GPP_{LP}}\right) - GPP_{NO2SP} - GPP_{NO2LP}$$

$$GPP_{SP} = GPP_{NO2SP} + GPP_{NH2SP}$$
$$GPP_{LP} = GPP_{NO2LP} + GPP_{NH2LP}$$

$$\frac{d(NH)}{dt} = DON2NH + PON2NH + RES_{SP} \times \left(1.0 - \frac{GPP_{NO2SP}}{GPP_{SP}}\right) + RES_{LP} \times \left(1.0 - \frac{GPP_{NO2LP}}{GPP_{LP}}\right) + EXR_{SZ} + EXR_{LZ} + EXR_{PZ} - NIT - GPP_{NH2SP} - GPP_{NH2LP}$$

$$\frac{d(SI)}{dt} = OP2SI + (RES_{LP} - GPP_{NO2LP} + GPP_{NH2LP}) \times R_{SN}$$

$$\frac{d(DON)}{dt} = PON2DON + EXC_{SP} + EXC_{LP} - DON2NH$$

$$\frac{d(PON)}{dt} = MOR_{SP} + MOR_{LP} + MOR_{SZ} + MOR_{LZ} + MOR_{PZ} + EGE_{SZ} + EGE_{LZ} + EGE_{PZ} - PON2NH - PON2DON \pm SINK_{PON}$$

$$\frac{d(OP)}{dt} = (MOR_{LP} + GRA_{LP2LZ} + GRA_{LP2PZ}) \times R_{SN} - OP2SI \pm SINK_{OP}$$

<u>Small phytoplankton terms expanded:</u>

Limitation Terms:

$$TL_{SP} = \exp(Q_{VSP} \times \theta)$$

$$NL_{SP} = \frac{NO}{NO + K_{NO2SP}}$$

$$AL_{SP} = \frac{NH}{(NH + K_{NH2SP})\left(1.0 + \frac{NH}{K_{NH2SP}}\right)}$$

$$LL_{SP} = \left(1 - \exp\left(\frac{\alpha_{SP} \times PAR}{V_{SP}}\right)\right) \times \exp\left(\frac{-\beta_{SP} \times PAR}{V_{SP}}\right)$$

$$GPP_{NO2SP} = V_{SP} \times TL_{SP} \times NL_{SP} \times LL_{SP} \times SP$$

$$GPP_{NH2SP} = V_{SP} \times TL_{SP} \times AL_{SP} \times LL_{SP} \times SP$$

$$RES_{SP} = R_{SP} \times exp(Q_{RSP} \times \theta) \times SP$$

$$MOR_{SP} = M_{SP} \times exp(Q_{MSP} \times \theta) \times SP$$

$$EXC_{SP} = E_{SP} \times (GPP_{NO2SP} + GPP_{NH2SP})$$

Large phytoplankton terms expanded:

Limitation Terms:

$$TL_{LP} = \exp(Q_{VLP} \times \theta)$$

$$NL_{LP} = \frac{NO}{NO + K_{NO2LP}}$$

$$AL_{LP} = \frac{NH}{(NH + K_{NH2LP})\left(1.0 + \frac{NH}{K_{NH2LP}}\right)}$$

$$SL_{LP} = \frac{SI}{SI + K_{SI}}$$

$$LL_{LP} = \left(1 - \exp(\frac{\alpha_{LP} \times PAR}{V_{LP}})\right) \times \exp\left(\frac{-\beta_{LP} \times PAR}{V_{LP}}\right)$$

$$\frac{SL}{TNL_{LP}} = \min\left[1.0, \frac{SI}{SI + K_{SI}} \Big/ \left(\frac{NO}{NO + K_{NO2LP}} + \frac{NH}{(NH + K_{NH2LP})\left(1.0 + \frac{NH}{K_{NH2LP}}\right)}\right)\right]$$

$$GPP_{NO2LP} = V_{LP} \times TL_{LP} \times NL_{LP} \times \frac{SL}{TNL_{LP}} \times LL_{LP} \times LP$$

$$GPP_{NH2LP} = V_{LP} \times TL_{LP} \times AL_{LP} \times \frac{SL}{TNL_{LP}} \times LL_{LP} \times LP$$

$$RES_{LP} = R_{LP} \times exp(Q_{RLP} \times \theta) \times LP$$

$$MOR_{LP} = M_{LP} \times exp(Q_{MLP} \times \theta) \times LP$$

$$EXC_{LP} = E_{LP} \times (GPP_{NO2LP} + GPP_{NH2LP})$$

Small zooplankton terms expanded:

Limitation Terms:

$$TL_{SZ} = \exp(Q_{GSZ} \times \theta)$$

$$GL_{SP2SZ} = \max\left[0.0, \left(1.0 - \exp\left(-\varphi_{SP2SZ} \times (\tau_{SP2SZ} - SP)\right)\right)\right]$$

$$GRA_{SP2SZ} = G_{SP2SZ} \times TL_{SZ} \times GL_{SP2SZ} \times SZ$$

$$MOR_{SZ} = M_{SZ} \times \exp(Q_{MSP} \times \theta) \times SP$$

$$EXR_{SZ} = GRA_{SP2SZ} \times (AE_{SZ} - GGE_{SZ})$$

$$EGE_{SZ} = GRA_{SP2SZ} \times (1.0 - AE_{SZ})$$

Large zooplankton terms expanded:

Limitation Terms:

$$TL_{LZ} = \exp(Q_{GLZ} \times \theta)$$

$$GL_{SP2SZ} = \max\left[0.0, \left(1.0 - \exp\left(\varphi_{LP2LZ} \times (\tau_{LP2LZ} - LP)\right)\right)\right]$$

$$GL_{SP2SZ} = \max\left[0.0, \left(1.0 - \exp\left(\varphi_{SZ2LZ} \times (\tau_{SZ2LZ} - SZ)\right)\right)\right]$$

$$GRA_{LP2LZ} = G_{LP2LZ} \times TL_{LZ} \times GL_{LP2LZ} \times LZ$$

$$GRA_{SZ2LZ} = G_{SZ2LZ} \times TL_{LZ} \times GL_{SZ2LZ} \times LZ$$

$$MOR_{SZ} = M_{LZ} \times \exp(Q_{MLZ} \times \theta) \times LZ$$

$$EXR_{SZ} = (GRA_{LP2LZ} + GRA_{SZ2LZ}) \times (AE_{LZ} - GGE_{LZ})$$

$$EGE_{SZ} = (GRA_{LP2LZ} + GRA_{SZ2LZ}) \times (1.0 - AE_{LZ})$$

Predatory zooplankton terms expanded:

Limitation Terms:

$$TL_{PZ} = \exp(Q_{GPZ} \times \theta)$$

$$GL_{LP2PZ} = \max\left[0.0, \left(1.0 - \exp\left(\varphi_{LP2PZ} \times (\tau_{LP2PZ} - LP)\right) \times \exp(-\lambda_{SZLZ} \times (SZ + LZ))\right)\right]$$

$$GL_{SZ2PZ} = \max\left[0.0, \left(1.0 - \exp\left(\varphi_{SZ2PZ} \times (\tau_{SZ2PZ} - SZ)\right) \times \exp(-\lambda_{LZ} \times (LZ))\right)\right]$$

$$GL_{LZ2PZ} = \max\left[0.0, \left(1.0 - \exp\left(\varphi_{LZ2PZ} \times (\tau_{LZ2PZ} - LZ)\right)\right)\right]$$

$$GRA_{LP2PZ} = G_{LP2PZ} \times TL_{PZ} \times GL_{LP2PZ} \times PZ$$

$$GRA_{SZ2PZ} = G_{SZ2PZ} \times TL_{PZ} \times GL_{SZ2PZ} \times PZ$$

$$GRA_{LZ2PZ} = G_{LZ2PZ} \times TL_{PZ} \times GL_{LZ2PZ} \times PZ$$

$$MOR_{PZ} = M_{PZ} \times \exp(Q_{MPZ} \times \theta) \times PZ^2$$

$$EXR_{PZ} = (GRA_{LP2PZ} + GRA_{SZ2PZ} + GRA_{LZ2PZ}) \times (AE_{PZ} - GGE_{PZ})$$

$$EGE_{PZ} = (GRA_{LP2PZ} + GRA_{SZ2PZ} + GRA_{LZ2PZ}) \times (1.0 - AE_{PZ})$$

Implicit bacterial rates terms expanded:

$$NIT = B_{NIT} \times exp(Q_{IBR} \times \theta) \times NH$$

$$PON2DON = B_{PON2DON} \times exp(Q_{IBR} \times \theta) \times PON$$

$$PON2NH = B_{PON2NH} \times exp(Q_{IBR} \times \theta) \times PON$$

$$DON2NH = B_{DON2NH} \times exp(Q_{IBR} \times \theta) \times DON$$

$$OP2SI = B_{OP2SI} \times exp(Q_{IBR} \times \theta) \times OP$$

Sinking of PON and OP:

$$SINK_{PON} = \frac{\omega \times \Delta t}{V_k} \times \left(\frac{PON_{K-1} \times V_{K-1}}{\Delta Z_{k-1}} - \frac{PON_k \times V_K}{\Delta Z_k}\right)$$

$$SINK_{OP} = \frac{\omega \times \Delta t}{V_k} \times \left(\frac{OP_{K-1} \times V_{K-1}}{\Delta z_{k-1}} - \frac{OP_k \times V_K}{\Delta z_k}\right)$$

Variable C:Chl model (Li et al., 2010):

$$V_{SPc} = V_{SP} \times TL_{SP} \times (NL_{SP} + AL_{SP}) \times \frac{\alpha_{SP}}{a_{SP} + \beta_{SP}} \times \left(\frac{\beta_{SP}}{a_{SP} + \beta_{SP}}\right)^{\beta_{SP}/\alpha_{SP}}$$

$$V_{LPc} = V_{LP} \times TL_{LP} \times (NL_{LP} + AL_{LP}) \times \frac{SL}{TNL_{LP}} \times \frac{\alpha_{LP}}{a_{LP} + \beta_{LP}} \times \left(\frac{\beta_{LP}}{a_{LP} + \beta_{LP}}\right)^{\beta_{LP}/\alpha_{LP}}$$

$$Chl2C_{SP} = ChlC_{SPmax} \Big/ \left(1.0 + \frac{ChlC_{SPmax} \times \alpha_{chl} \times PAR}{2.0 \times V_{SPc}}\right)$$

$$Chl2C_{LP} = ChlC_{LPmax} \Big/ \left(1.0 + \frac{ChlC_{LPmax} \times \alpha_{chl} \times PAR}{2.0 \times V_{LPc}}\right)$$

$$Chl_{SP} = SP \times \frac{C}{N} \times \frac{1.0\ mol\ C}{1000\ mmol\ C} \times \frac{12.011\ g\ C}{1.0\ mol\ C} \times \frac{1000\ mg\ C}{1.0\ g\ C} \times \max(Chl2C_{SP}, Chl2C_{SPmin})$$

$$Chl_{LP} = LP \times \frac{C}{N} \times \frac{1.0\ mol\ C}{1000\ mmol\ C} \times \frac{12.011\ g\ C}{1.0\ mol\ C} \times \frac{1000\ mg\ C}{1.0\ g\ C} \times \max(Chl2C_{LP}, Chl2C_{LPmin})$$

References

Damien, P., Pasqueron de Fommervault, O., Sheinbaum, J., Jouanno, J., Camacho-Ibar, V. F. and Duteil, O.: Partitioning of the Open Waters of the Gulf of Mexico Based on the Seasonal and Interannual Variability of Chlorophyll Concentration, J. Geophys. Res. Ocean., 123(4), 2592–2614, doi:10.1002/2017JC013456, 2018.

Fennel, K., Wilkin, J., Levin, J., Moisan, J., O'Reilly, J. and Haidvogel, D.: Nitrogen cycling in the Middle Atlantic Bight: Results from a three-dimensional model and implications for the North Atlantic nitrogen budget, Global Biogeochem. Cycles, 20(3), 1–14, doi:10.1029/2005GB002456, 2006.

Fennel, K., Hetland, R., Feng, Y. and Dimarco, S.: A coupled physical-biological model of the Northern Gulf of Mexico shelf: Model description, validation and analysis of phytoplankton variability, Biogeosciences, 8(7), 1881–1899, doi:10.5194/bg-8-1881-2011, 2011.

Gomez, F. A., Lee, S. K., Liu, Y., Hernandez, F. J., Muller-Karger, F. E. and Lamkin, J. T.: Seasonal patterns in phytoplankton biomass across the northern and deep Gulf of Mexico: A numerical model study, Biogeosciences, 15(11), 3561–3576, doi:10.5194/bg-15-3561-2018, 2018.

Kishi, M. J., Kashiwai, M., Ware, D. M., Megrey, B. a., Eslinger, D. L., Werner, F. E., Noguchi-Aita, M., Azumaya, T., Fujii, M., Hashimoto, S., Huang, D., Iizumi, H., Ishida, Y., Kang, S., Kantakov, G. a., Kim, H. C., Komatsu, K., Navrotsky, V. V., Smith, S. L., Tadokoro, K., Tsuda, A., Yamamura, O., Yamanaka, Y., Yokouchi, K., Yoshie, N., Zhang, J., Zuenko, Y. I. and Zvalinsky, V. I.: NEMURO-a lower trophic level model for the North Pacific marine ecosystem, Ecol. Modell., 202(1–2), 12–25, doi:10.1016/j.ecolmodel.2006.08.021, 2007.

Li, Q. P., Franks, P. J. S., Landry, M. R., Goericke, R. and Taylor, A. G.: Modeling phytoplankton growth rates and chlorophyll to carbon ratios in California coastal and pelagic ecosystems, J. Geophys. Res. Biogeosciences, 115(4), 1–12, doi:10.1029/2009JG001111, 2010.

Brzezinski, M. A. (1985), The Si: C: N ratio of marine diatoms: interspecific variability and the effect of some environmental variables 1, *Journal of Phycology*, *21*(3), 347-357.

Stukel, M. R., K. A. S. Mislan, M. Décima, and L. Hmelo (2014), Detritus in the pelagic ocean, in *Eco-DAS IX Symposium Proceedings*, edited by P. F. Kemp, pp. 49-76, Association for the Sciences of Limnology and Oceanography.